J|A|C|S
ARTICLES
Published on Web 05/27/2006

A Family of Rare-Earth-Based Single Chain Magnets: Playing with Anisotropy

Kevin Bernot,[†,‡] Lapo Bogani,[†] Andrea Caneschi,[†] Dante Gatteschi,*[,†] and Roberta Sessoli[†]

Contribution from the La.M.M., Department of Chemistry and INSTM Research Unit, Università di Firenze, Via della Lastruccia 3, 50019, Sesto Fiorentino (FI), Italy, and Sciences Chimiques de Rennes, UMR 6226 CNRS-INSA Rennes, Equipe "Matériaux Inorganiques: Chimie Douce et Réactivité", INSA Rennes, 20 Avenue des buttes de Coësmes, CS 14315, 35043 Rennes Cedex, France

Received February 28, 2006; E-mail: dante.gatteschi@unifi.it

Abstract: The first family of rare-earth-based single chain magnets is presented. Compounds of general formula [M(hfac)$_3$(NITPhOPh)], where M = Eu, Gd, Tb, Dy, Ho, Er, or Yb, and PhOPh is the nitronyl−nitroxide radical (2,4′-benzoxo-4,4,5,5-tetramethylimidazoline-1-oxyl-3-oxide), have been structurally characterized and found to be isostructural. The characterization of both static and dynamic magnetic properties of the whole family is reported. Dy, Tb, and Ho compounds display slow relaxation of the magnetization, and *ac* susceptibility shows a thermally activated regime with energy barriers of 69, 45, and 34 K for Dy, Tb, and Ho compounds, respectively, while only a frequency-dependent susceptibility is observed for Er below 2.0 K. In Gd and Yb derivatives, antiferromagnetic interactions dominate. The pre-exponential factors differ by about 4 orders of magnitude. Finite size effects, due to naturally occurring defects, affect the static and dynamic properties of the compounds differently.

Introduction

While the synthesis of a new compound with unconventional properties is certainly a particularly appealing task, especially if following a rational design,[1] one goal of no less importance is the synthesis of whole families of systems, in which the properties can be tuned at will. Such studies, allowing comparison between similar systems, are powerful tools to rationalize the properties of the materials under study and often lead to further synthetic advances. This is particularly true for the field of molecular magnetism, where the systematic synthesis of families of compounds provided a clear indication of the patterns of magnetic interaction and allowed for the rationalization of the magnetic coupling mechanism.[2] With the discovery, about 15 years ago, of Single Molecule Magnets (SMMs), that is, molecular clusters that show slow relaxation of the magnetization at low temperature and give rise to magnetic hysteresis of molecular origin,[3] accompanied by important quantum effects,[4] the synthesis of families of related clusters has become an important topic and is still a rich field of research.[5] The further discovery, some years ago, of a superparamagnetic-like behavior in one-dimensional systems has opened new perspectives in the development of molecular magnets. The first of such systems, the molecular coordination polymer [Co(hfac)$_2$(NITPhOMe)][6] (where hfac = hexafluoroacetylacetonate and NITPhOMe = 2,4′-methoxo-4,4,5,5-tetramethylimidazoline-1-oxyl-3-oxide), showed hysteresis at temperatures significantly higher than those ever reached with SMMs and thus raised the hope of obtaining molecular materials for magnetic information storage and processing at accessible temperatures. Anyway, the development of such materials has been somewhat hampered by the difficulty in combining the two strict requirements needed to observe the desired behavior, that is, a strong Ising anisotropy of the magnetic centers and very weak interchain interactions. Although a number of different polymeric systems showing this

[†] Università di Firenze.
[‡] INSA Rennes.

(1) (a) St-Pierre, G.; Chagnes, A.; Bouchard, N.-A.; Harvey, P. D.; Brossard, L.; Menard, H. *Langmuir* **2004**, *20*, 6365. (b) Evans, O.; Lin, W. *Chem. Mater.* **2001**, *13*, 3009. (c) Descalzo, A. B.; Rurack, K.; Weisshoff, H.; Martinez-Manez, R.; Marcos, M. D.; Amoros, P.; Hoffmann, K.; Soto, J. *J. Am. Chem. Soc.* **2005**, *127*, 184.
(2) (a) Willet, R. D.; Gatteschi, D.; Kahn, O. *Magneto-Structural Correlations in Exchange Coupled Systems*; Reidel Publishing: Dordrecht, The Netherlands, 1983. (b) Kahn, O. *Molecular Magnetism*; VCH: New York, 1993.
(3) See, for a review: Gatteschi, D.; Sessoli, R. *Angew. Chem.* **2003**, *115*, 278; *Angew. Chem., Int. Ed.* **2003**, *42*, 268.
(4) (a) Thomas, L.; Lionti, F.; Ballou, R.; Gatteschi, D.; Sessoli, R.; Barbara, B. *Nature* **1996**, *383*, 145. (b) Friedman, J. R.; Sarachik, M. P.; Tejada, J.; Ziolo, R. *Phys. Rev. Lett.* **1996**, *76*, 3830. (c) Wernsdorfer, W.; Sessoli, R. *Science* **1999**, *284*, 133. (d) Wernsdorfer, W.; Aliaga-Alcade, N.; Hendrickson, D. N.; Christou, G. *Nature* **2002**, *416*, 406.
(5) (a) King, P.; Wernsdorfer, W.; Abboud, K. A.; Christou, G. *Inorg. Chem.* **2004**, *43*, 7315. (b) Andres, H.; Basler, R.; Gudel, H. U.; Aromi, G.; Christou, G.; Buttner, H.; Ruffle, B. *J. Am. Chem. Soc.* **2000**, *122*, 12469. (c) Rajaraman, G.; Murugesu, M.; Sanudo, E. C.; Soler, M.; Wernsdorfer, W.; Helliwell, M.; Muryn, C.; Raftery, J.; Teat, S.; Christou, G.; Brechin, E. K. *J. Am. Chem. Soc.* **2004**, *126*, 15445. (d) Yoo, J.; Brechin, E. K.; Yamaguchi, A.; Nakano, M.; Huffman, J. C.; Maniero, A. L.; Brunal, L.-C.; Awaga, K.; Ishimoto, H.; Christou, G.; Hendrickson, D. N. *Inorg. Chem.* **2000**, *39*, 3615. (e) Boskovic, C.; Brechin, E. K.; Streib, W. E.; Folting, K.; Bollinger, J. C.; Hendrickson, D. N.; Christou, G. *J. Am. Chem. Soc.* **2002**, *124*, 3725. (f) Aromi, G.; Knapp, M. J.; Claude, J.-P.; Huffman, J. C.; Hendrickson, D. N.; Christou, G. *J. Am. Chem. Soc.* **1999**, *121*, 5489. (g) Castro, S. L.; Sun, Z.; Grant, C. M.; Bollinger, J. C.; Hendrickson, D. N.; Christou, G. *J. Am. Chem. Soc.* **1998**, *120*, 2365.
(6) Caneschi, A.; Gatteschi, D.; Lalioti, N.; Sangregorio, C.; Sessoli, R.; Venturi, G.; Vindigni, A.; Rettori, A.; Pini, M. G.; Novak, M. A. *Angew. Chem.* **2001**, *113*, 1810; *Angew. Chem., Int. Ed.* **2001**, *40*, 1760.

behavior has been synthesized and studied,[7] collectively called, as a class of compounds, Single Chain Magnets (SCMs),[8] up to now, only one family of such systems is known.[9] The archetype [Co(hfac)$_2$NITPhOMe], which was based on the metal−radical approach strategy,[10] has not led to the creation of a family of systems with tunable properties yet, mainly due to the rather poor reactivity of the Co(II) metallic center.

Rare-earth radical-based chains are very appealing candidates for SCMs, due to the Ising anisotropy often encountered in these metal ions.[11] Moreover, the very similar chemical properties of lanthanides allow for the easy substitution of the metallic center. Our approach thus consists of exploiting these characteristics of lanthanides, together with the engineering possibilities opened by the "radical-as-ligand" strategy. Careful design of the nitronyl−nitroxide radical (2,4′-benzoxo-4,4,5,5-tetramethylimidazoline-1-oxyl-3-oxide), NITPhOPh, allowed us to obtain magnetically isolated chains containing lanthanide centers stabilized by intrachain supramolecular interactions.[12] The efficacy of this strategy was previously reported for the chain compound [Dy(hfac)$_3$(NITPhOPh)], **1**,[12] which is the first successful attempt at obtaining a SCM using rare-earth ions and the first example of how to rationally modify the ligand to design a SCM from materials known to undergo three-dimensional ordering.[13] This compound exhibits all features of a superparamagnetic system, and a hysteresis loop opens below 3 K. These dynamical features are accompanied by a very rich static behavior with the presence of several low energy states. This result has also opened the possibility of studying the interplay between SCM behavior and the possible presence of slow relaxation of single rare-earth magnetic centers, as evidenced in recent works.[14]

In this work, we exploit the chemical possibilities opened by the creation of a rare-earth-based SCM family in which the magnetic center, and thus the anisotropy, can be tuned. It must be stressed that, in all other reported SCMs, the substitution of the metallic site leads to structural changes, and thus, the only other SCM family available is based on the substitution of the ligands around the metal centers.[9] Here we describe a whole family of isostructural chain compounds with the formula [M(hfac)$_3$(NITPhOPh)], where M = Eu, Gd, Tb, Dy, Ho, Er, or Yb. A complete characterization of the magnetic behavior of the family of compounds is presented, and both static and dynamic properties are discussed and analyzed. By comparing static and dynamic properties, we evidence the interplay of anisotropy and SCM behavior, and we show that, in some cases, the chains are to be assigned to a dynamical regime dominated by finite size effects.

Experimental Section

General Procedures and Materials. All chemical and solvents used were reagent grade. Syntheses of the starting material, radical NITPhOPh, have been performed according to literature methods.[15]

Synthesis of [M(hfac)$_3$(NITPhOPh)]. The reacting salts [M(hfac)$_3$·2H$_2$O] (where M = Eu, Gd, Tb, Dy, Ho, Er, or Yb) were synthesized using the following procedure: 1.78 mL (24 mmol) of a 25% ammonia solution was added dropwise to 3.39 mL (24 mmol) of hfac in 100 mL of ether at 2 °C. Then 8 mmol of [M(Cl)$_3$·5H$_2$O] in 10 mL of water was added to the solution. After half an hour of strong stirring, 20 mL of water was added. Then organic and aqueous phases were separated and washed with water and ether, respectively. The organic phase was dried on magnesium sulfate, filtered, and then concentrated to form a yellowish oil; 20 mL of hexane was then added, and the solution was then heated to 55 °C for some minutes. After filtration, to separate the formed solid, the compound was kept in freezer at −15 °C, where it crystallized. The mean overall yield was about 40%.

All the polymeric systems [M(hfac)$_3$NITPhOPh] were synthesized by the following procedure: 1 mmol of [M(hfac)$_3$·2H$_2$O] was dissolved in 30 mL of dry boiling *n*-heptane. The solution was left to boil for 20 min and then cooled to 75 °C, when 1 mmol of the crystalline solid radical NITPhOPh was then slowly added under stirring and 3 mL of CH_2Cl_2 was added. The final solution was then cooled to room temperature and was left still for about 24 h to give dark needle-like crystals suitable for X-ray analysis. Elemental analysis calculated for $C_{34}H_{24}O_9N_2F_{18}Eu$: C, 37.17; H, 2.20; O, 13.11. Found: C, 37.11; H, 2.22; O, 13.13. Calcd (%) $C_{34}H_{24}O_9N_2F_{18}Gd$: C, 37.00; H, 2.19; O, 13.05. Found: C, 36.98; H, 2.17; O, 13.08. Calcd (%) $C_{15}H_7O_8F_{18}Tb$: C, 36.94; H, 2.19; O, 13.03. Found: C, 36.95; H, 2.23; O, 13.02. Calcd (%) $C_{34}H_{24}O_9N_2F_{18}Ho$: C, 36.74; H, 2.18; O, 12.96. Found: C, 36.70; H, 2.20; O, 12.92. Calcd (%) $C_{34}H_{24}O_9N_2F_{18}Er$: C, 36.66; H, 2.17; O, 12.93. Found: C, 36.63; H, 2.14; O, 12.89. Calcd (%) $C_{34}H_{24}O_9N_2F_{18}Yb$: C, 36.47; H, 2.16; O, 12.86. Found: C, 36.51; H, 2.13; O, 12.82.

All compounds were found to melt in a very narrow temperature range at 134 ± 0.3 °C and immediately after they decompose to a reddish slimy substance.

Physical Measurements. Temperature dependent *dc* magnetic susceptibility measurements were performed on solid polycrystalline samples with a Cryogenic Ltd. S600 SQUID magnetometer and were all corrected for the diamagnetic contribution, as calculated with Pascal's constants, and for the diamagnetism of the sample holder, as independently determined. All magnetization curves were measured with an Oxford VSM system after inclusion in Apiezon grease to prevent orientation of the crystallites. Data were corrected for the magnetism of the grease, which was independently determined at the same temperature and fields. The *ac* magnetic susceptibility was measured using a homemade probe operating in the 55−25000 Hz range.[16] Powder diffraction patterns were recorded on a powder

(7) (a) Lescouezec, R.; Vaissermann, J.; Ruiz-Perez, C.; Lloret, F.; Carrasco, R.; Julve, M.; Verdaguer, M.; Dromzee, Y.; Gatteschi, D.; Wernsdorfer, W. *Angew. Chem.* **2003**, *115*, 1521; *Angew. Chem., Int. Ed.*, **2003**, *42*, 1483. (b) Liu, T.; Fu, D.; Gao, S.; Zhang, Y.; Sun, aH.; Su, G.; Liu, Y. *J. Am. Chem. Soc.* **2003**, *125*, 13976. (c) Toma, L. M.; Lescouezec, R.; Lloret, F.; Julve, M.; Vaissermann, J.; Verdaguer, M. *Chem. Commun.* **2003**, 1850. (d) Pardo, E.; Ruiz-Garcia, R.; Lloret, F.; Faus, J.; Julve, M.; Journaux, Y.; Delgado, F.; Ruiz-Perez, C. *Adv. Mater.* **2004**, *16*, 1597. (e) Maignan, A.; Hardy, V.; Hebert, S.; Drillon, M.; Lees, M. R.; Petrenko, O.; Paul, D. M.; Khomskii, D. *J. Mater. Chem.* **2004**, *14*, 1231. (f) Ferbinteanu, M.; Miyasaka, H.; Wernsdorfer, W.; Nakata, K.; Sugiura, K.; Yamashita, M.; Coulon, C.; Clerac, R. *J. Am. Chem. Soc.* **2005**, *127*, 3090. (g) Costes, J. P.; Clemente-Juan, J. M.; Dahan, F.; Milon, J. *Inorg. Chem.* **2004**, *43*, 8200. (h) Toma, L. M.; Lescouëzec, R.; Pasàn, J.; Ruiz-Pérez, C.; Vaissermann, J.; Cano, J.; Carrasco, R.; Wersndorfer, W.; Lloret, F.; Julve, M. *J. Am. Chem. Soc.* **2006**, *128*, in press (doi:10.1021/ja058030v).

(8) Clerac, R.; Miyasaka, H.; Yamashita, M.; Coulon, C. *J. Am. Chem. Soc.* **2002**, *124*, 12837.

(9) Miyasaka, H.; Clerac, R.; Mizushima, K.; Sugiura, K.; Yamashita, M.; Wernsdorfer, W.; Coulon, C. *Inorg. Chem.* **2003**, *42*, 8203.

(10) (a) Caneschi, A.; Gatteschi, D.; Rey, P. *Prog. Inorg. Chem.* **1991**, *39*, 331. (b) Luneau, D.; Rey, P. *Coord. Chem. Rev.* **2005**, *249*, 2591 and references therein.

(11) (a) Carlin, R. L. *Magnetochemistry*; Springer-Verlag: New York, 1986. (b) Abraham, A.; Bleaney, B. *Electron Paramagnetic Resonance of Transition Ions*; Dover: New York, 1986.

(12) Bogani, L.; Sangregorio, C.; Sessoli, R.; Gatteschi, D. *Angew. Chem., Int. Ed.* **2005**, *44*, 5817. X-ray crystallographic file (CIF) for the Dy compound, CCDC 262704, can also be obtained free of charge from the Cambridge Crystallographic Data Centre (e-mail: deposit@ccdc.cam.ac.uk).

(13) Benelli, C.; Caneschi, A.; Gatteschi, D.; Sessoli, R. *Adv. Mater.* **1992**, *4*, 504.

(14) (a) Giraud, R.; Wernsdorfer, W.; Tkachuk, A. M.; Mailly, D.; Barbara, B. *Phys. Rev. Lett.* **2001**, *87*, 057203. (b) Ishikawa, N.; Sugita, M.; Ishikawa, T.; Koshihara, S.; Kaizu, Y. *J. Am. Chem. Soc.* **2003**, *125*, 8694. (c) Ishikawa, T.; Sugita, M.; Wernsdorfer, W. *J. Am. Chem. Soc.* **2005**, *127*, 3650. (d) Ishikawa, T.; Sugita, M.; Wernsdorfer, W. *Angew. Chem.* **2003**, *117*, 2991; *Angew. Chem., Int. Ed.* **2005**, *44*, 2931.

(15) Ullman, E. F.; Osiecki, J. H.; Boocock, D. G. B.; Darcy, R. *J. Am. Chem. Soc.* **1972**, *94*, 7049.

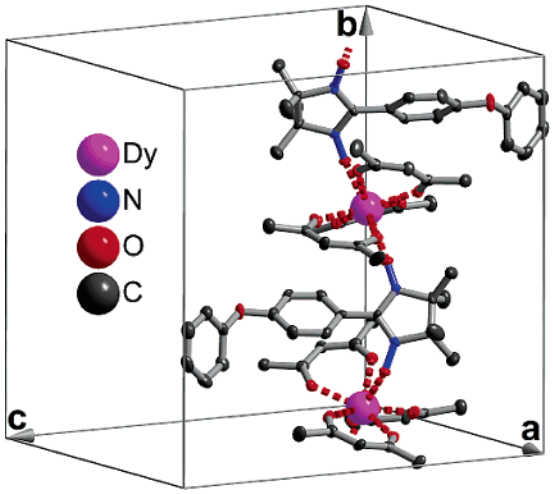

Figure 1. View of the crystal structure of [Dy(hfac)$_3$NITPhOPh], at 150 K. Fluorine and hydrogen atoms were omitted for clarity. Coordination bonds are represented as segmented. All other chains are found to be isostructural.

diffractometer Bruker D8 Avance working with Cu Kα radiation in $\theta/2\theta$ mode. Powder diffraction pattern of Dy compound was simulated from a CIF file using PowderCell software. FT-IR spectra were recorded on a Perkin-Elmer Spectrum BX spectrometer in KBr pellets. Melting points were recorded on a Büchi B-545 apparatus on microcrystalline samples.

Crystallography. Crystallographic measurement on Dy compound, depicted in Figure 1, has already been reported.[12] Cell determinations of [M(hfac)$_3$NITPhOPh] (with M = Eu, Gd, Tb, Dy, Ho, Er, or Yb) were performed on the same apparatus. The family crystallizes in the orthorhombic space group $P2_12_12_1$ (No. 19). Main structural data are reported in Table 1.

Results

Synthesis and Structural Description. As the chemical reactivity of the lanthanides used is basically the same,[17] all polymeric systems were synthesized in the same way, following a slight modification of the synthesis reported for **1**. In our study, we always used the same radical, so as to obtain isostructural systems. The structure of **1** (shown in Figure 1) and its underlying synthetic strategy were previously described.[12]

Briefly, the compound is formed by chains, parallel to the *b* crystallographic axis of octacoordinated M(hfac)$_3$ centers connected via radical units, which act as bis-monodentate ligands. The bonds between the metal center and the two oxygen atoms of the bridging radicals were found to be very close to one another (2.385(6) and 2.358(4) Å) and can thus be expected to give similar magnetic exchange. As it was observed in other metal NIT(R) derivatives,[18] stacking interactions between the inner aromatic ring of the spacer and an hfac ligand, which can be clearly identified,[19] play a major role in stabilizing the polymeric form of the compound. We then chose to favor them by activating the aromatic part of the radical using an ether group as a substituent. The outer aromatic ring of the radical, on the contrary, acts as a spacer and is placed between the chains and is found in a niche between two other chains, surrounded by the fluorine atoms of four hfac ligands. The spacers of two different chains alternatively occupy the free volume between the chains, then minimizing even the possible weak magnetic interactions between the radicals.

In our study of the effect of the substitution of the rare-earth ion on the magnetic properties, we focused on synthesizing a family of materials using rare earths with very different anisotropies. Starting from our previous results, we mainly focused on the elements around Dy and after Gd, but to check if structural changes took place with elements before Gd, we also synthesized a chain with Eu, finding that it is isostructural. Cell determinations were performed on all lanthanide derivatives, and the cell parameters found are given in Table 1.

As a further proof that the chains are isostructural, powder diffraction patterns were recorded for all compounds. Except for a small difference in the degree of crystallinity, all compounds show the same diffraction pattern, in good agreement with that simulated from the CIF file of the Dy compound. These results confirm not only that the compounds are isostructural with no incidence of lanthanide contraction[17] but also that other polymorphs are not present (see Supporting Information).

FT-IR Analysis. All compounds display the same spectra as Ln−O bond vibrations are not visible in the investigated range. The Tb compound spectrum, together with a list and assignment of main peaks, is available in the Supporting Information.

Static Magnetic Properties. Polycrystalline powder SQUID measurements of all compounds were recorded at temperatures between 2 and 300 K. The χT products versus temperature are shown in Figures 2−6 for all the new compounds, while data for the Dy chain have been previously reported. The main parameters found are summarized in Table 2, together with data for the Dy chain, to allow easy comparison. It can be seen that all compounds display a room temperature susceptibility slightly lower than that expected for noninteracting spins, but in very good agreement with previously reported data.[20] For many lanthanides, a decrease in the χT value on decreasing temperature, due to single ion anisotropy, is expected, and all of our compounds except the Gd chain display, at relatively high temperature, a decrease due to this fact. The magnetization versus temperature curves, also reported in Figures 2−6, were obtained on polycrystalline samples with a VSM system. All measurements were performed on samples included in Apiezon grease to avoid orientation effects with the field and were acquired continuously while the field was sweeping at 12 kOe/min from 120 to −120 kOe.

The measurements performed on the Gd compound are shown in the lower part of Figure 2. The SQUID measurement shows a χT value at room temperature of 8.2 emu·K/mol, only slightly lower than the value expected for one Gd(III) ion, which has a $^8S_{7/2}$ ground state, plus an uncoupled $S = 1/2$ radical center. This fact is anyhow in agreement with previous reports.[20] The value remains roughly constant until about 35 K, where an abrupt decrease is clearly visible, reaching a value of 2.1 emu·K/mol at 2 K. The magnetization versus field measurement,

(16) Midollini, S.; Orlandini, A.; Rosa, P.; Sorace, L. *Inorg. Chem.* **2005**, *44*, 2060.
(17) Moeller, T.; Martin, D. F.; Thompson, L. C.; Ferrus, R.; Feistel, G. R.; Randall, W. J. *Chem. Rev.* **1965**, *65*, 1.
(18) Caneschi, A.; Gatteschi, D.; Lalioti, N.; Sangregorio, C.; Sessoli, R. *J. Chem. Soc., Dalton Trans.* **2000**, 3907.
(19) Janiack, C. *J. Chem. Soc., Dalton Trans.* **2000**, 3885.
(20) (a) Benelli, C.; Gatteschi, D. *Chem. Rev.* **2002**, *102*, 2369. (b) Benelli, C.; Gatteschi, D.; Caneschi, A.; Sessoli, R. *Inorg. Chem.* **1993**, *32*, 4797. (c) Benelli, C.; Caneschi, A.; Gatteschi, D.; Sessoli, R. *J. Appl. Phys.* **1993**, *73*, 5333. (d) Benelli, C.; Caneschi, A.; Gatteschi, D.; Pardi, L.; Rey, P. *Inorg. Chem.* **1990**, *29*, 4223.

Table 1. Cell Axes (Å), Angles (deg), and Volume (Å^3) as Determined for All Chain Compounds at 298 K

chain compound	*a*	*b*	*c*	α	*β*	*γ*	volume
[Eu(hfac)$_3$(NITPhOPh)]	14.468(4)	16.757(6)	17.127(4)	89.98(2)	90.05(2)	90.12(2)	4152.4
[Gd(hfac)$_3$(NITPhOPh)]	14.437(8)	16.70(1)	17.130(9)	90.01(5)	89.85(4)	89.86(5)	4130.9
[Tb(hfac)$_3$(NITPhOPh)]	14.453(5)	16.67(1)	17.094(6)	90.07(4)	89.96(3)	89.73(4)	4119.8
[Dy(hfac)$_3$(NITPhOPh)][a]	14.441(6)	16.713(9)	17.140(7)	90.13(4)	90.00(4)	90.28(3)	4140.85
[Ho(hfac)$_3$(NITPhOPh)]	14.422(5)	16.65(1)	17.083(6)	90.28(3)	89.95(3)	90.13(4)	4103.4
[Er(hfac)$_3$(NITPhOPh)]	14.389(3)	16.661(8)	17.104(3)	89.94(2)	90.00(1)	89.87(2)	4101.1
[Yb(hfac)$_3$(NITPhOPh)]	14.389(2)	16.739(7)	17.102(3)	90.20(2)	89.92(1)	89.77(2)	4119.7

[a] The cell values reported here are taken at room temperature and thus slightly differ from those previously published[12] recorded at 150 K.

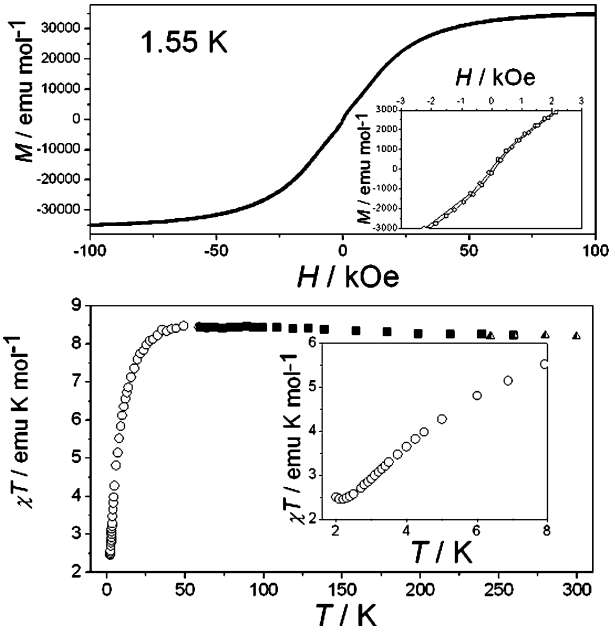

Figure 2. Magnetic data recorded for the [Gd(hfac)$_3$(NITPhOPh)] chain as a polycrystalline sample. (Top) Magnetization versus field measurement at 1.55 K and with a field sweep rate of 12 kOe/min. In the inset, we show an enlargement of the low field region. (Bottom) Temperature dependence of the χT product from SQUID magnetic measurements. Symbols are experimental data (empty circles are recorded in an external field of 0.1 kOe, squares in 1 kOe, and half-filled triangles in 10 kOe). In the inset, we show the low temperature dependence of the χT product.

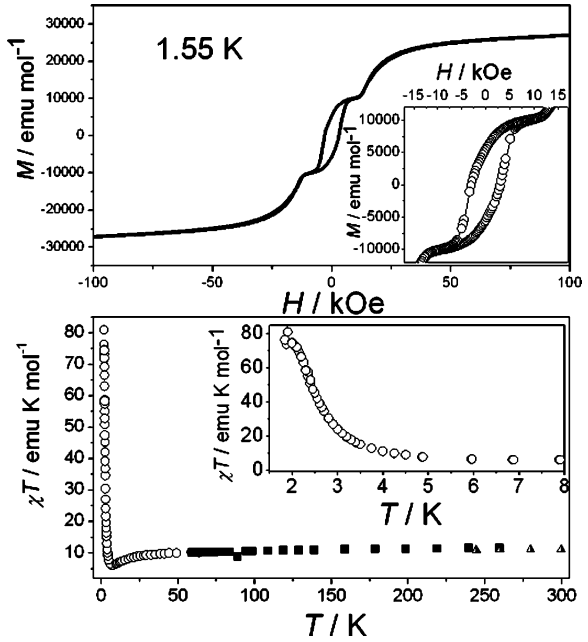

Figure 3. Magnetic data recorded for the [Tb(hfac)$_3$(NITPhOPh)] chain as a polycrystalline sample. (Top) Magnetization versus field measurement at 1.55 K and with a field sweep rate of 12 kOe/min. In the inset, we show an enlargement of the low field region. (Bottom) Temperature dependence of the χT product from SQUID magnetic measurements. Symbols are experimental data (empty circles are recorded in an external field of 0.1 kOe, squares in 1 kOe, and half-filled triangles in 10 kOe). In the inset, we show the low temperature dependence of the χT product.

reported in the upper part of Figure 2, does not show any hysteresis, but a very slight kink is visible between −500 and 500 Oe. The magnetization value at 120 kOe is found to be 35625 emu/mol (6.38 μ_B) at 1.55 K.

The temperature dependence of the χT product for the Tb compound (lower part of Figure 3) displays a very different behavior. The room temperature χT value, 11.1 emu·K/mol, lower than that expected for the $^7F_6$ state of Tb(III) plus an uncoupled $S = 1/2$ radical, is in agreement with previously reported data for similar compounds.[20a] This value remains almost unchanged down to 50 K, where a slow decrease is visible, reaching a minimum of 6.08 emu·K/mol at 6.9 K. Below this temperature, the χT product increases markedly and it reaches a value of 81 emu·K/mol at 1.89 K.

The magnetization versus field curve at 1.45 K (upper part of Figure 3) shows a hysteretic behavior. Rather interestingly, while the Dy chain shows the presence of a small step very close to zero field, indicating some kind of antiferromagnetic interaction in the system, the Tb compound shows no sign of this antiferromagnetic ground state, and the opening of the hysteresis is more clearly visible. The coercive field was found to be 3 kOe, while the remnant magnetization was found to amount to 5500 emu/mol. The magnetization value was 26 700 emu/mol (4.78 μ_B) at 120 kOe and 1.55 K. A well-defined step at 13.7 kOe, with a value of 10 000 emu/mol, was observed in this case.

The χT versus T measurements performed on the Ho compound (lower part of Figure 4) show a room temperature value of 14.4 emu·K/mol, again lower than the value theoretically expected for a $^5I_8$ ground state plus an uncoupled $S = 1/2$. This value decreases smoothly on decreasing the temperature and reaches a minimum value of 4.89 emu·K/mol at 4.5 K. Then the curve rapidly increases and reaches a round maximum at 2.25 K with a value of 8.50 emu·K/mol. The magnetization versus field measurement (upper part of Figure 4) shows no hysteresis. Nevertheless, some slight steps are visible between 2 and 9 kOe for a median value of 5000 emu/mol, while the magnetization reaches 34 300 emu/mol (6.14 μ_B) at 120 kOe and 1.55 K.

The χT versus T curve for the Er compound (lower part of Figure 5) resembles that of the Tb one. The room temperature χT value is 11.37 emu·K/mol, lower than the expected for a $^4I_{15/2}$ ground state plus an uncoupled $S = 1/2$ radical center. χT decreases smoothly and reaches a minimum value of 7.16 emu·

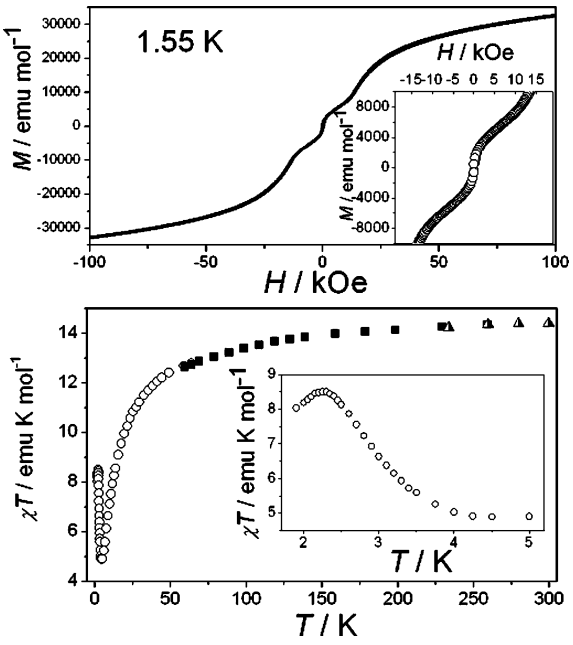

Figure 4. Magnetic data recorded for the [Ho(hfac)$_3$(NITPhOPh)] chain as a polycrystalline sample. (Top) Magnetization versus field measurement at 1.55 K and with a field sweep rate of 12 kOe/min. In the inset, we show an enlargement of the low field region. (Bottom) Temperature dependence of the χT product from SQUID magnetic measurements. Symbols are experimental data (empty circles are recorded in an external field of 0.1 kOe, squares in 1 kOe, and half-filled triangles in 10 kOe). In the inset, we show the low temperature dependence of the χT product.

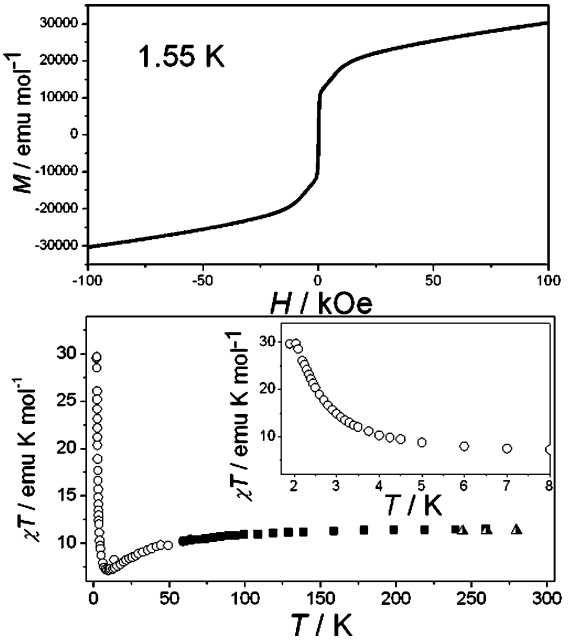

Figure 5. Magnetic data recorded for the [Er(hfac)$_3$(NITPhOPh)] chain as a polycrystalline sample. (Top) Magnetization versus field measurement at 1.55 K and with a field sweep rate of 12 kOe/min. In the inset, we show an enlargement of the low field region. (Bottom) Temperature dependence of the χT product from SQUID magnetic measurements. Symbols are experimental data (empty circles are recorded in an external field of 0.1 kOe, squares in 1 kOe, and half-filled triangles in 10 kOe). In the inset, we show the low temperature dependence of the χT product.

K/mol at 10.0 K. Then a maximum is rapidly reached at 2.05 K with a value of 29.72 emu·K/mol as shown in the inset. The magnetization versus field measurement (shown in the upper part of Figure 5) does not display any significant hysteresis. A

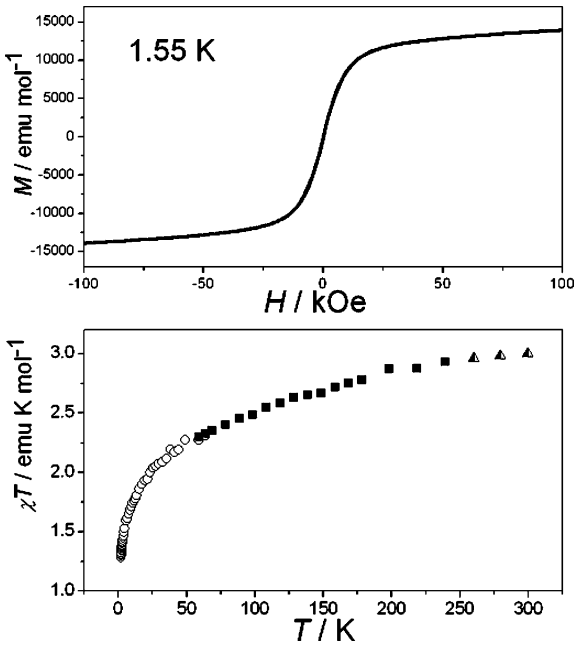

Figure 6. Magnetic data recorded for the [Yb(hfac)$_3$(NITPhOPh)] chain as a polycrystalline sample. (Top) Magnetization versus field measurement at 1.55 K and with a field sweep rate of 12 kOe/min. (Bottom) Temperature dependence of the χT product from SQUID magnetic measurements. Symbols are experimental data (empty circles are recorded in an external field of 0.1 kOe, squares in 1 kOe, and half-filled triangles in 10 kOe).

Table 2. Main Magnetic Data Extracted from the Static Properties of the Chain Compounds

rare earth	χT, 300 K (emu·K/mol)	M, 120 kOe (emu/mol)	step field (kOe)	steepness, step (emu·mol^{-1}·Oe^{-1})	slope (SI) (K)
Gd	8.20	35625	N.A	N.A.	N.A.
Tb	11.10	26700	13.77	1310	9.1 ± 0.5
Dy[b]	12.2	30900	16.23	1680	18.2 ± 0.3
Ho	14.4	34300	13.08	1080	3.4 ± 0.3
Er	11.37	32000	6.26	790	4.6 ± 0.2
Yb	3.00	14300	N.A.	N.A.	N.A.

[a] The step field value and its steepness are extracted from the first derivatives of the magnetization curves. the slope is extracted from the logarithmic scaling of the χT curves. [b] Parameters extracted from data reported in ref 12.

very slight modification of the trend of the curves is visible around 5 kOe with a value of about 15 000 emu/mol. The highest value of the magnetization is 32 000 emu/mol (5.73 μ_B) at 120 kOe and 1.55 K.

The last χT versus T measurements (performed on the Yb compound and reported in Figure 6) show a room temperature value of 3.00 emu·K/mol, and this is slightly lower than that expected for a $^2I_{7/2}$ ground state plus an uncoupled $S = 1/2$. In this case, a monotonic decrease down to 1.28 emu·K/mol at 2 K is observed on lowering the temperature. The magnetization versus field measurement (upper part of Figure 6) shows no steps and no hysteresis. The saturation value of the magnetization, about 14300 emu/mol (2.56) at 1.55 K, is found to be, as predicted,[11] significantly smaller than those of the previous compounds.

It can be easily seen that, similarly to the Dy compound, the Tb, Ho, and Er chains display a step in the magnetization curves at different field values and with different steepness. As in the case of the Dy compound, all these features were found to be independent of the field sweep rate and only become smoother

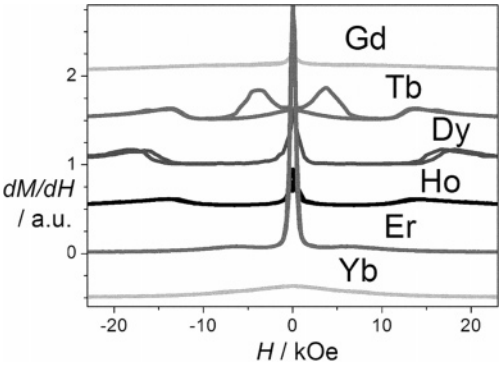

Figure 7. Derivatives of the magnetization curves for the Gd, Tb, Dy, Ho, Er, and Yb chains. Magnetization curves were all recorded at 1.55 K and with a field sweep rate of 12 kOe/min. The first peak observed for the Tb compound around 5 kOe is obviously due to the hysteresis.

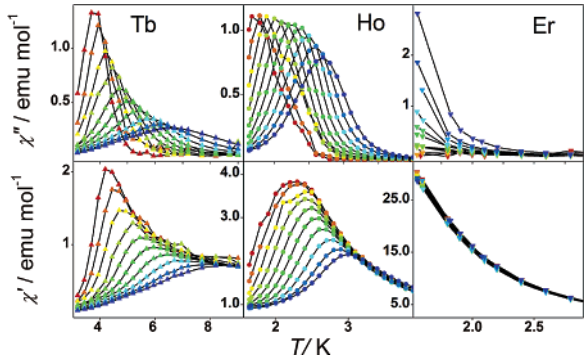

Figure 8. Temperature dependence of the imaginary χ'' (top) and real χ' (bottom) components of the *ac* susceptibility measured in zero applied field for 10 logarithmically spaced frequencies in range of 110 Hz (red) to 20 000 Hz (blue). Lines are guides to the eye.

on increasing the temperature. It is interesting to note that they are found also above the temperature at which the hysteresis is observed. To better appreciate the differences, the first derivatives of all the magnetization curves shown in Figures 2−6 are displayed in Figure 7, translated with an arbitrary offset for the sake of clarity. The position, taken as the fields of the maxima of the derivative, and the steepness and the peak value of the steps are reported in Table 2, along with all the main experimental parameters. The position of the steps is increasing proceeding from Tb to Dy (for which it reaches a maximum value of ca. 16 kOe), whereas it continuously decreases from Dy to Yb. A similar trend is observed also for the steepness.

Dynamic Magnetic Properties. Zero-field-cooled and field-cooled (ZFC−FC) curves were recorded on polycrystalline samples of all systems, as a preliminary analysis of the dynamical properties, but, in contrast to what was observed for the Dy chain, no difference was detected between the two curves down to 1.9 K.

Then *ac* susceptibility was measured down to 1.5 K and in the frequency range of 55−25000 Hz. No out-of-phase signal was observed for the Gd and Yb compounds. The remaining Tb, Ho, and Er chains, on the contrary, all showed some form of slow relaxation of the magnetization, as found in **1**. The temperature dependence of the in-phase χ' and out-of-phase χ'' signals, recorded in zero static field, is reported in Figure 8 for the three compounds. The Tb chain is clearly the one which shows a χ'' signal at higher temperatures. All peaks in χ'' are found above 3 K, while the χ' signal has an increasing value on lowering the frequency and the curves are superimposable above 9 K to the *dc* one. The frequency-dependent χ'' signal is found at lower temperature, below 3.5 K, in the Ho chain, and the height of its maximum tends to saturate below 2.25 K, in correspondence to the maximum in the static χT curve. For the Er chain, the frequency dependence of the signal is visible only at the lowest temperatures available, and this prevented the extraction of the dynamical parameters.

Discussion

Static Magnetic Properties. The largely unquenched orbital contributions associated with the ground states of the lanthanides make the simulation of the data very difficult. In most cases, anyway, low symmetry components of the crystal field remove the degeneracy, leaving one Kramers doublet lying lowest, separated from the excited states by some tens of cm^{-1}. It is usually a reasonable approximation to treat the Dy(III) and Er(III) ions at low temperature as an effective $S = 1/2$, corresponding to the Kramers doublet, with high anisotropy.[11] On the contrary, Tb(III) and Ho(III) ions are usually considered as $S = 1$ spin centers, with considerable anisotropy.[11] Yb(III) shows a significantly smaller magnetic anisotropy, while Gd(III) is substantially isotropic. We can immediately notice that for the more isotropic ions, Gd and Yb, the magnetic behavior is dominated by AF interactions even if a ferrimagnetic behavior would be expected due to the alternation of different magnetic moments. It is, however, well-known that compounds involving nitronyl−nitroxide radicals and rare-earths ions show the simultaneous presence of both nearest-neighbor (NN) and next-nearest-neighbor (NNN) exchange interactions between the magnetic centers, these last ones are antiferromagnetic in nature.[20] When the anisotropy is small, the magnetic energy is minimized in a helical arrangement of the spins that can result in a decrease of the χT product.[21] In the case of Ising-type anisotropy, the magnetic moments are forced in one direction and the helical arrangement that compensates the magnetic moments cannot be attained. Ferrimagnetic behavior is therefore expected to prevail and is indeed observed. Although a detailed analysis is not possible in these complex systems, given also the low symmetry environment around the metal ions, an indication on the kind of magnetic anisotropy of the chains can be gained by performing a scaling procedure of the temperature dependence of the susceptibility.[22] In fact, the susceptibility of the ferromagnetic Ising chain shows an exponential behavior of the χT product, $\chi T \propto e^{2J/k_B T}$, where J is the exchange energy between nearest-neighbors (NN), thus including the product of the alternating spins. Plotting the logarithm of χT versus the inverse of the temperature should afford a straight line, and the slope directly provides the exchange energy.

We want to stress here that the exponential divergence is observed only when the geometrical length of the chains exceeds the correlation length, ξ, originated by the intrachain exchange interaction. If naturally occurring defects cut the chains in segments with an average distance between two breaks that is much smaller than ξ, χT does not further increase on lowering T but approaches a constant value.

(21) (a) Benelli, C.; Sessoli, R.; Rettori, A.; Pini, M. G.; Bartolomé, F.; Bartolomé, J. *J. Magn. Magn. Mater.* **1995**, 1649. (b) Pini, M. G.; Rettori, A. *Phys. Rev. B* **1993**, 3240. (c) Harada, I. *J. Phys. Soc. Jpn.* **1984**, 1643.
(22) (a) Coulon, C.; Clerac, R.; Lecren, L.; Wernsdorfer, W.; Miyasaka, H. *Phys. Rev. B* **2004**, *69*, 132408. (b) Ferbinteanu, M.; Miyasaka, H.; Wernsdorfer, W.; Nakata, K.; Sugiura, K.; Yamashita, M.; Coulon, C.; Clerac, R. *J. Am. Chem. Soc.* **2005**, *127*, 3090.

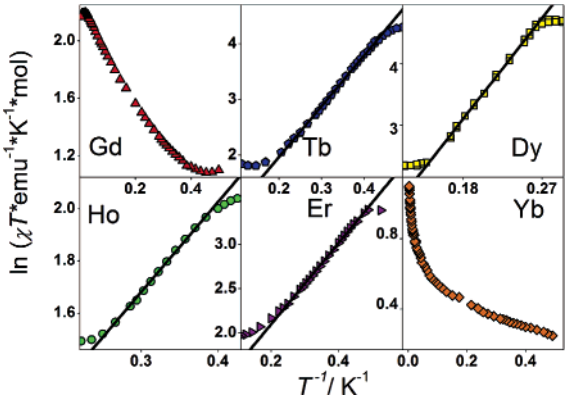

Figure 9. Scaling of the data for all the compounds using an Ising temperature dependence of the susceptibility (see text) and plotting $\ln(\chi T \cdot \text{mol} \cdot \text{K}^{-1} \cdot \text{emu}^{-1})$ versus $1/T$. Data for Tb (blue pentagons), Dy (yellow squares), Ho (green circles), and Er (violet triangles) compounds display the predicted scaling behavior, and the corresponding fits to the regions with the linear regime are shown as gray lines. The behavior of Gd (red triangles) and Yb (orange rhomboids) compounds does not agree with the scaling procedure.

As mentioned above, this scaling procedure cannot be applied for Gd, which shows a dominant AF behavior. Fitting of the data, performed in the temperature range between 45 and 10 K with a Curie−Weiss law, as shown in the Supporting Information ($R = 0.9996$), affords a Weiss temperature $\theta = 5.6$ K. This indicates that NNN antiferromagnetic interactions dominate as interactions between Gd and nitronyl−nitroxides and are known to be ferromagnetic.[20,23] The leveling of χT observed at very low temperature can be rationalized with the expected helical arrangement of the spins with the angle formed by similar spins (Gd−Gd or Rad−Rad) that is close to, but not exactly, π.

For the Tb chain, the scaling procedure gave a straight line, as shown in Figure 9, for the temperature range between 5.6 and 2.2 K. Below this temperature, finite size effects become important and produce a deviation from the linear regime.[24] Linear regression performed on the data of the linear region gave $R = 0.9994$ and a slope $= 9.1 \pm 0.5$ K. This indicates a mainly Ising behavior and, in the interplay between NN and NNN couplings, dominant ferromagnetic interactions. Such a behavior is in agreement with data available in the literature, which report a rather strong Ising anisotropy of the ion, with g_z values around 17, even greater than those of Dy, and vanishing $g_\perp$.[11]

The results obtained for the Dy compound have already been discussed,[12] but to allow easy comparison with the results on the other chains, we report the results of the scaling procedure in Figure 9 and the main parameters in Table 2. It is to be noted that the temperature range in which the scaling procedure is valid is between 8.6 and 3.7 K, shifted to higher temperatures compared to that of the Tb chain. Again, below this temperature, finite size effects are expected.

The Ho compound also shows a rather clear indication of Ising anisotropy, again in agreement with the behavior reported in the literature,[11] as shown in Figure 9. The linear regime is, however, found at lower temperatures, and fitting of the data was performed between 3.9 and 2.5 K, obtaining $R = 0.999$ and a much lower slope $= 3.4 \pm 0.3$ K. The deviation from the straight line observed below 2.5 K is, however, accompanied by a decrease in the χT curve, as shown in Figure 4. This cannot be due only to finite size effects but rather to the population at low temperature of a less magnetic state as a consequence of competing NN and NNN interactions, which in this compound are almost perfectly balanced.

The Er chain gave satisfactory rescaling of the data on a straight line in a slightly wider temperature range, spanning between 4.2 and 2.1 K. EPR studies on the behavior of Er-based compounds evidenced either an XY behavior or a mild Ising anisotropy,[11] depending on the ligand field around the metal center. Linear regression gave an agreement factor $R = 0.9996$ and slope $= 4.6 \pm 0.2$ K, which is in agreement with a close balancing of NN and NNN couplings.

Eventually, the behavior of the Yb strongly resembles that of Gd(III) with dominating AF interactions. This is in agreement with earlier reports of almost isotropic behavior of the Yb(III) ions.[11] Interestingly, also the step in the magnetization curve seems to correlate with the magnetic anisotropy. The presence of the step, peculiarity of these rare-earth−NIT-R chains, could be tentatively associated with a field-induced crossover between states with different alignment of the magnetic moments. Those states are close in energy as a result of the competition of NN and NNN interactions. According to this picture, the realignment of the magnetic moments is expected to occur smoothly in isotropic extended systems but abruptly when discrete magnetic states are present as in the ideal Ising system. Indeed, a well-defined step has been experimentally observed in our investigation only for the anisotropic metal ions.

The static properties of this family of chain systems indicate that four out of six compounds have the prerequisites to display Glauber dynamics. The Gd and Yb compounds, in agreement with the literature, were found to lack the necessary requirement of Ising anisotropy of the magnetic centers. The fact that the rescaling procedure was possible in different temperature ranges indicates that the compounds have very different anisotropies, which become appreciable at different temperature ranges.

Dynamic Magnetic Properties. The idea that Ising-type magnetic anisotropy can influence the relaxation of purely one-dimensional magnets was first theoretically suggested by Glauber in the 1960s.[25] Although the physics of real systems is somewhat more complicated, giving birth to new and very interesting phenomena, this theory is still the basis of the explanation of the slow relaxing behavior observed in SCMs. In all systems reported in the literature, a frequency-dependent peak in the *ac* susceptibility was observed, and below a blocking temperature, T_b, the dynamics of the magnetization reversal becomes slower than the time of the experiment, giving rise to a hysteresis loop and a difference between the Zero-Field-Cooled and the Field-Cooled curves. According to Glauber's theory, an Ising chain shows exponential divergence of the relaxation time of the magnetization on decreasing the temperature, $\tau = \tau_0 e^{\Delta k_B T}$ with $\Delta = 4J$, where J, as stated above, corresponds to the NN exchange energy and includes the product of the interacting spins. The temperature dependence of the relaxation

(23) (a) Benelli, C.; Caneschi, A.; Gatteschi, D.; Pardi, L. *Inorg. Chem.* **1992**, *31*, 741. (b) Sutter, J. P.; Kahn, M. L.; Golhen, S.; Ouahab, L.; Kahn, O. *Chem.—Eur. J.* **1998**, *4*, 571. (c) Kahn, M. L.; Sutter, J. P.; Golhen, S.; Guionneau, P.; Ouahab, L.; Kahn, O.; Chasseau, D. *J. Am. Chem. Soc.* **2000**, *122*, 3413.

(24) Bogani, L.; Sessoli, R.; Pini, M. G.; Rettori, A.; Novak, M. A.; Rosa, P.; Massi, M.; Fedi, M. E.; Guintini, L.; Caneschi, A.; Gatteschi, D. *Phys. Rev. B* **2005**, *72*, 064406.

(25) Glauber, R. J. *J. Math. Phys.* **1963**, *4*, 294.

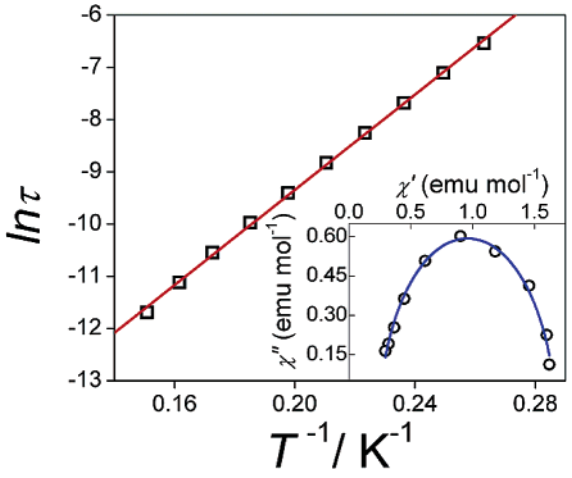

Figure 10. Arrhenius plot extracted for the [Tb(hfac)$_3$(NITPhOPh)] chain. Linear regression performed on the data gave a $\tau_0 = (9.6 \pm 0.4) \times 10^{-9}$ s and an energy barrier $\Delta = 45 \pm 1$ K with an $R = 0.9995$. Squares represent data points, and the line is the fit to the data. (Inset) Argand diagram taken at 4.95 K in the frequency range of 110 Hz to 20 kHz. Circles are the experimental points, while the line represents a fitting with an extended Debye model with $\alpha = 0.10 \pm 0.03$ and $R^2 = 0.999$.

time then depends on an energy barrier proportional to the exchange coupling constant and to the spin values and on a prefactor parameter τ_0 that represents the flipping rate of an isolated spin.

Finite size effects that limit the low-temperature divergence of χT also affect the dynamic properties.[24,26] When the correlation length exceeds the geometrical length of the chains, the process of relaxation starts at one end of the segment with a halved energy cost.[27] The energy barrier thus becomes $\Delta = 2J$ with a crossover between the two dynamic regimes that has been indeed observed for the Dy chain, as well as for a Mn(III)−Fe(III) chain.[7f]

Data for the Tb compound (reported in the left part of Figure 8) are a clear signature of SCM behavior. From the position of the maximum of the imaginary component of the susceptibility, χ'', we extracted the relaxation time, defined as $\tau(T_{max}) = 1/(2\pi\nu)$. Plotting these data as $\ln(\tau)$ versus $1/T$ and fitting them using the Arrhenius law afforded the plot depicted in the upper part of Figure 10. No trace of crossover, contrary to what found for the Dy chain, can be identified. Linear fit of the data ($R = 0.9998$) gave an activation energy Δ of 45 ± 1 K and a τ_0 value of $(9.6 \pm 0.4) \times 10^{-9}$ s. This latter parameter is rather long, in perfect agreement with a superparamagnetic-like character of the relaxation dynamics. The barrier, on the contrary, is smaller than that in the Dy chain. The absence of the crossover is in agreement with the observation of finite size effects on the rescaling plot only below the temperature range investigated with the *ac* susceptibility measurements. As the peak temperatures used to extract the Arrhenius law are much higher than those of the deviation from the linear regime in the rescaling plot of Figure 9, we can exclude that finite size effects are affecting the dynamics. We can also notice that, in the temperature range where the dynamical features are observed (around 5 K), the correlation length, calculated as e^{Sl/k_BT}, using the slope, Sl, of the rescaling procedure is around 6 spins, much shorter than the expected average distance between two naturally occurring defects. The system has then to be considered in the infinite limit, contrary to what was observed in the CoPhOMe compound, where the much stronger exchange interaction leads to a rapid increase of ξ.[24]

The extracted Argand plot (as depicted in the bottom part of Figure 10) could be fitted with an extended Debye model for the whole temperature range investigated, by use of the following relation:[28]

$$\chi(\omega) = \chi_S + \frac{\chi_T - \chi_S}{1 + (i\omega\tau)^{1-\alpha}}$$

where χ_T is the isothermal susceptibility, χ_S the adiabatic susceptibility, ω is the frequency of the *ac* field, and τ is the relaxation time of the system at the temperature at which the fit is performed. The fitting procedure gave good agreement at all temperatures (the worst value found for R^2 was 0.987) and afforded an always identical α value of 0.10 ± 0.01. This value is in good agreement with previously reported values for other SCMs[7] and suggests a very narrow distribution of relaxation times, close to a single relaxation time, as expected for superparamagnetic-like dynamics. It must be noted that a rather high value of χ_T, about 0.29 ± 0.05 emu/mol, was found at all temperatures. This indicates that the system is not wholly affected by the slow relaxing dynamics: there are parts of it that can follow the alternating field. This can be ascribed for powder sample to transversal components of the magnetization that are free to relax fast and can thus follow the alternating field of the *ac* experiments.

The Dy data were already reported and discussed,[12] but the main dynamical parameters are summarized in Table 3 for easy comparison. Briefly, the Arrhenius law showed the presence of a crossover at 3.7 K, interpreted as the passage between the infinite and finite size regimes. Indeed, this is the temperature at which the scaling procedure shows important finite size effects.

Data for the Ho compound are less straightforward to interpret. The χ'' signal shows the presence of some crossover around 2.25 K. The Arrhenius diagram for the compound, extracted as for the previous chains, is depicted in the upper part of Figure 11.

A slight kink is visible around 2.25 K, but the limited temperature range spanned by the data prevents a sure interpretation of this feature. Separate fitting of both the low- and high-temperature data was anyway possible, as shown in Figure 11. Fitting of the low-temperature region ($R = 0.9991$) gave a slope $\Delta' = 18 \pm 2$ K and a pre-exponential factor $\tau'_0 = (4.4 \pm 0.6) \times 10^{-8}$ s, while the high-temperature region was well fitted ($R = 0.993$) with a slope $\Delta'' = 34 \pm 2$ K and $\tau''_0 = (2.6 \pm 0.5) \times 10^{-11}$ s. Both prefactors are physically sound values for the flipping rate of an isolated spin. The fact that the τ_0 increases in the low-temperature regime, instead of decreasing, indicates that we are not in the presence of a crossover to a Spin Glass-like dynamics.[29] Moreover, the spacing between the peaks obtained at different, logarithmically spaced, frequencies does not decrease, as one would expect in the case of a system where

(26) Bogani, L.; Caneschi, A.; Fedi, M.; Gatteschi, D.; Massi, M.; Novak, M. A.; Pini, M. G.; Rettori, A.; Sessoli, R.; Vindigni, A. *Phys. Rev. Lett.* **2004**, *92*, 207204.
(27) Dasilva, J. K. L.; Moreira, A. G.; Soares, M. S.; Barreto, F. C. S. *Phys. Rev. E* **1995**, *52*, 4527.
(28) Cole, K. S.; Cole, R. H. *J. Chem. Phys.* **1941**, *9*, 341.
(29) Mydosh, J. A. *Spin Glasses: An Experimental Introduction*; Taylor & Francis Ltd.: London, 1993.

Table 3. Main Magnetic Data Extracted from the Dynamic Properties of the Chain Compounds[a]

rare earth	SI (K)	Δ' (K)	τ'_0 (s)	Δ'' (K)	τ''_0 (s)	α
Tb	9.1 ± 0.5	N.A.	N.A.	45 ± 1	$(9.6 \pm 0.4) \times 10^{-9}$	0.10 ± 0.03
Dy[b]	18.2 ± 0.3	42 ± 1	$(5.6 \pm 0.4) \times 10^{-10}$	69 ± 1	$(1.9 \pm 0.4) \times 10^{-12}$	0.16 ± 0.01
Ho	3.4 ± 0.3	18 ± 2	$(4.4 \pm 0.5) \times 10^{-8}$	34 ± 2	$(2.6 \pm 0.6) \times 10^{-11}$	0.22 ± 0.07
Er	4.6 ± 0.2	N.A.	N.A.	N.A.	N.A.	N.A.

[a] The barrier (Δ) and attempt time values (τ_0) were extracted from fitting of the Arrhenius plots. The superscripts ($'$) and ($''$) were adopted to indicate parameters in the finite size and infinite regimes, respectively. The values of α were obtained from fitting of the Argand plots with an extended Debye model (see text). [b] Parameters extracted from data reported.[12]

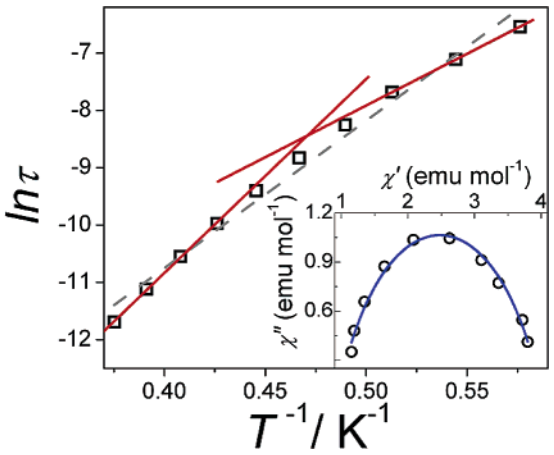

Figure 11. Arrhenius plot extracted for the [Ho(hfac)$_3$(NITPhOPh)] chain. Linear regression performed on data between 2.7 and 2.35 K gave a $\tau''_0 = (2.6 \pm 0.4) \times 10^{-11}$ s and an energy barrier $\Delta'' = 34 \pm 2$ K with an $R = 0.9991$. Linear regression of the low-temperature region (1.7−2.1 K) gave $\tau'_0 = (4.4 \pm 0.4) \times 10^{-8}$ s and $\Delta' = 18 \pm 2$ K with an $R = 0.993$. Squares are data points, black lines the two fits, and the gray line is a tentative fit to all the points. (Inset) Argand diagram taken at 2.4 K (circles) in the frequency range of 110 Hz to 20 kHz. Circles are the experimental points, while the line represents fitting with an extended Debye model with $\alpha = 0.22 \pm 0.07$ and $R^2 = 0.998$.

three-dimensional interactions are becoming important. The passage from the infinite to finite size regimes, as observed in the Dy chain, could be supported by the almost exact halving of the barrier; however, it must be noted that its value is significantly larger than that estimated from the scaling of the χT curve. Moreover, the crossover temperature coincides with the maximum in the static χT curve.

The extracted Argand plots, shown in the inset of Figure 11, could be fitted with an extended Debye model in the whole temperature range (worst $R^2 = 0.989$). Such fittings gave a α mean value of 0.22 ± 0.07 that remained almost unvaried in the whole temperature range accessible to us. A slight decreasing trend, at the limit of the sensibility of the extraction procedure, was observed on lowering the temperature from 2.6 K ($\alpha = 0.27 \pm 0.04$) to 1.9 K ($\alpha = 0.20 \pm 0.03$), which is again the contrary of what was expected for a Spin Glass or a system close to three-dimensional ordering.[29] An even higher value of the χ_S parameter was found, around 1.15 emu/mol, suggesting that the transverse components free to follow the alternating field are here more important.

Data recorded for the Er compound did not allow for reliable extraction of the relevant parameters of the dynamics, but clearly show a much faster relaxation, even if the slope extracted from the scaling procedure of Figure 9 is higher than that of the preceding Ho analogue. On the other hand, the temperature at which slow relaxation becomes observable also depends on the pre-exponential factor τ_0.

We notice in Table 3 that this parameter ranges over ca. 4 orders of magnitude, being largest for Tb and smallest for Dy. In SMMs, the value of this parameter has been linked to the availability of suitable low-energy phonon states that allow for the reversal of the magnetization and has been shown to depend on the fifth power of the sound speed in the system.[30] In our isostructural family, the speed of sound is expected to be constant; and therefore, the wide variation in τ_0 has to be attributed to the electronic properties of the rare-earth ions.

The definition of a blocking temperature is not unambiguous as directly related to the time window of the experimental technique. In *ac* experiments, we notice that the blocking temperature decreases in the order Tb, Dy, Ho, Er, confirming the key role played by the pre-exponential factor in the investigated temperature range. This trend parallels that observed in the magnetic anisotropy and is in agreement with previous observation in lanthanide−phthalocyanine SMMs.[14b] For longer time scales, which correspond to lower temperatures, the largest exchange interaction observed in the Dy derivative dominates.

Concluding Remarks

In this study, we have presented the second ever family of single chain magnet compounds. The creation of such groups of systems is clearly important to obtain insights into the parameters that can affect the relaxing behavior and then to tune them so as to observe slow magnetic relaxation at higher temperature. The family of chain compounds reported in this paper is the first based on rare earths and has the unprecedented characteristics of allowing easy substitution of the magnetic center. Thanks to this synthetic advance, we could investigate the variation of the magnetic properties as a function of the anisotropy of the metal centers. The only chains to display a SCM behavior were those with clear signatures of Ising anisotropy, as predicted.

The comparison of the energy barrier estimated by *ac* susceptometry to the slope in the scaling procedure of the χT curves shows that the former is always significantly larger than the latter. Therefore, the relaxation mechanism in this family of SCMs is not well described by the simple Glauber model. It appears that an additional contribution is present that can be associated with the relaxation of the single ion. This mechanism has been already proposed[7f] for SCMs based on a Mn(III)−Fe(III)−Mn(III) trimeric unit that, on its own, behaves indeed as a SMM with its own energy barrier δ. The total barrier has been in first approximation assumed to be $\Delta = 2J + \delta$ or $\Delta = 4J + \delta$, depending if the system is in the finite size regime or not, respectively.[22]

Monomeric species of anisotropic rare-earth ions in a high symmetry environment have recently been widely investigated

(30) Villain, J.; Hartmann-Boutron, F.; Sessoli, R.; Rettori, A. *Europhys. Lett.* **1994**, *27*, 159.

because they show SMM behavior with very high energy barrier for the reversal of the magnetization.[14] In this study, we have shown that by using rare earths to build SCMs the single ion contribution to the energy barrier can significantly compensate the weak exchange interaction that characterizes 4*f* ions. Moreover, the wide variability of the pre-exponential τ_0 factor, observed in this isostructural family, evidences its key role in the magnetization dynamics of this class of materials. By means of a rationalization of this parameter, up to now very poorly investigated, a sensible increase in the blocking temperature could be obtained. The analysis of the dynamic properties of the rare-earth building units of these chains, that is, monomeric species showing a similar coordination environment, is the next step toward a deeper understanding of the slow relaxation in one-dimensional materials.

Acknowledgment. We gratefully acknowledge Dr. M. G. Pini for critical revision of the manuscript and stimulating discussions. The authors thank the Laboratoire Matériaux Inorganiques: Chimie Douce et Réactivité, INSA Rennes, and in particular Prof. O. Guillou. We also thank Prof. A. Rettori for helpful discussion, and Dr. C. Sangregorio and Dr. S. Ciattini for help with structural characterization. We acknowledge financial support from Italian MURST (FIRB and PRIN grants), from the EC through the Human Potential Program RTN-QUEMOLNA (MRTN-CT-2003-504880), from the NE-MAG-MANET (NMP3-CT-2005-515767), and from German DFG (SPP1137).

Supporting Information Available: Additional magnetic data for [Gd(hfac)$_3$NITPhOPh], FT-IR spectra for [Tb(hfac)$_3$-NITPhOPh], powder diffraction pattern for all compounds, superposition of [Dy(hfac)$_3$NITPhOPh] powder diffraction pattern, and simulated spectra from CIF file, and elemental analysis. This material is available free of charge via the Internet at http://pubs.acs.org.

JA061101L